Positive feedbacks promote power-law clustering of Kalahari vegetation

Todd M. Scanlon[1], Kelly K. Caylor[2], Simon A. Levin[3] & Ignacio Rodriguez-Iturbe[4]

The concept of local-scale interactions driving large-scale pattern formation has been supported by numerical simulations, which have demonstrated that simple rules of interaction are capable of reproducing patterns observed in nature[1,2]. These models of self-organization suggest that characteristic patterns should exist across a broad range of environmental conditions provided that local interactions do indeed dominate the development of community structure. Readily available observations that could be used to support these theoretical expectations, however, have lacked sufficient spatial extent or the necessary diversity of environmental conditions to confirm the model predictions. We use high-resolution satellite imagery to document the prevalence of self-organized vegetation patterns across a regional rainfall gradient in southern Africa, where percent tree cover ranges from 65% to 4%. Through the application of a cellular automata model, we find that the observed power-law distributions of tree canopy cluster sizes can arise from the interacting effects of global-scale resource constraints (that is, water availability) and local-scale facilitation. Positive local feedbacks result in power-law distributions without entailing threshold behaviour commonly associated with criticality. Our observations provide a framework for integrating a diverse suite of previous studies that have addressed either mean wet season rainfall or landscape-scale soil moisture variability as controls on the structural dynamics of arid and semi-arid ecosystems.

Scale is an essential factor in linking pattern and process[3], and an adequate characterization of tree canopy distributions must span scales ranging from that of individual to that of the landscape. Large-scale plot studies such as those at Barro Colorado Island and a limited number of other locations have proven to be extremely valuable for defining vegetation characteristics such as canopy gap distribution[1,4] and species-specific clustering[5]. The massive amount of manual sampling required to compile these data sets, however, places a practical limitation on their widespread collection. High-resolution remote sensing is an alternative for detecting landscape-level vegetation pattern, and one that is particularly well suited for monitoring sparse vegetation in which individual tree canopies can be distinguished[6]. The ease by which these data can be acquired allows for a more geographically widespread detection of large-scale spatial patterns.

Inferring process from vegetation pattern has been a fundamental motivation of many landscape ecological studies, yet unambiguous determination of the factors that generate and maintain patterns is often obfuscated by the existence of multiple mechanisms that can give rise to commonly observed spatial arrangements. For example, random patterns can be indicative of the absence of spatial interactions, but random patterns are also known to emerge from strong competitive interactions[7]. Aggregated patterns, such as those routinely observed for woody tree species in natural communities, have been attributed to the disparate mechanisms of dispersal limitation[8] and habitat differentiation[9]. It has been suggested that the identification of dominant processes that lead to emergent vegetation pattern could benefit from a more thorough statistical measure of the vegetation spatial structure that implicitly considers the broad range of spatial scales over which aggregation occurs, rather than simply characterizes the average aggregation tendency of individuals[10]. We adopt such an approach in applying cluster size analysis to tree canopy distributions and evaluate the consistency of the patterns over a range of environmental conditions.

Remote sensing analysis focuses on the Kalahari Transect in southern Africa, one in a number of worldwide International Geosphere-Biosphere Programme transects[11] that spans a mean annual rainfall gradient from approximately 1,200 to 200 mm per year. IKONOS satellite images were acquired for six locations along the Kalahari Transect during the 2000 wet season to augment concurrent field surveys, which have produced detailed information about the savanna vegetation[12,13]. Common to each of these locations is the homogeneous sand formation that underlies them (Supplementary Fig. 1), a feature that provides constant background spectral reflectance for remote sensing and acts as a normalizing factor for comparing rainfall–vegetation relationships between sites. A strong correlation ($r^2 = 0.84$, $n = 10$) exists between mean wet season rainfall ($\bar{r}$) and fractional tree cover (f_t), both established from ground-based measurements[12]. Key descriptors of the individual sites are listed in Table 1 and spatial arrangements of tree canopies derived from the IKONOS images are shown in Fig. 1a.

We describe the distribution of cluster sizes within each landscape using the inverse cumulative distribution, which is the probability that a cluster area (A) is greater than or equal to a, $P(A \geq a)$. To

Table 1 | Kalahari site characteristics

Site	Lat./Lon.	$\bar{r}$ (mm)	f_t	$\bar{c}$ (m²)	Dominant tree species
Mongu, Zambia	14.42° S, 23.52° E	879	0.65	14.4	*Brachystegia spiciformis*
Senanga, Zambia	15.86° S, 23.34° E	811	0.54	23.1	*Brachystegia spiciformis*
Pandamatanga, Botswana	18.66° S, 25.50° E	698	0.32	15.8	*Schinziophyton rautanenii, Baikiaea plurijuga*
Sandveld, Namibia	22.02° S, 19.17° E	409	0.19	3.3	*Terminalia sericea*
Tshane, Botswana	24.17° S, 21.89° E	365	0.14	10.3	*Acacia erioloba*
Vastrap, South Africa	27.75° S, 21.42° E	216	0.04	2.0	*Acacia erioloba*

Mean annual rainfall, $\bar{r}$, is extrapolated from nearby meteorological stations. Fractional tree cover, f_t, mean canopy area, $\bar{c}$, and the dominant species are derived from 0.25–1.0 ha stem map surveys of the sites[12,13]. Lat., latitude; Lon., longitude; S, south; E, east.

[1]Department of Environmental Sciences, University of Virginia Charlottesville, Virginia 22903, USA. [2]Department of Geography, Indiana University Bloomington, Indiana 47401, USA. [3]Department of Ecology & Evolutionary Biology, Princeton University Princeton, New Jersey 08544, USA. [4]Department of Civil and Environmental Engineering, Princeton University Princeton, New Jersey 08544, USA.
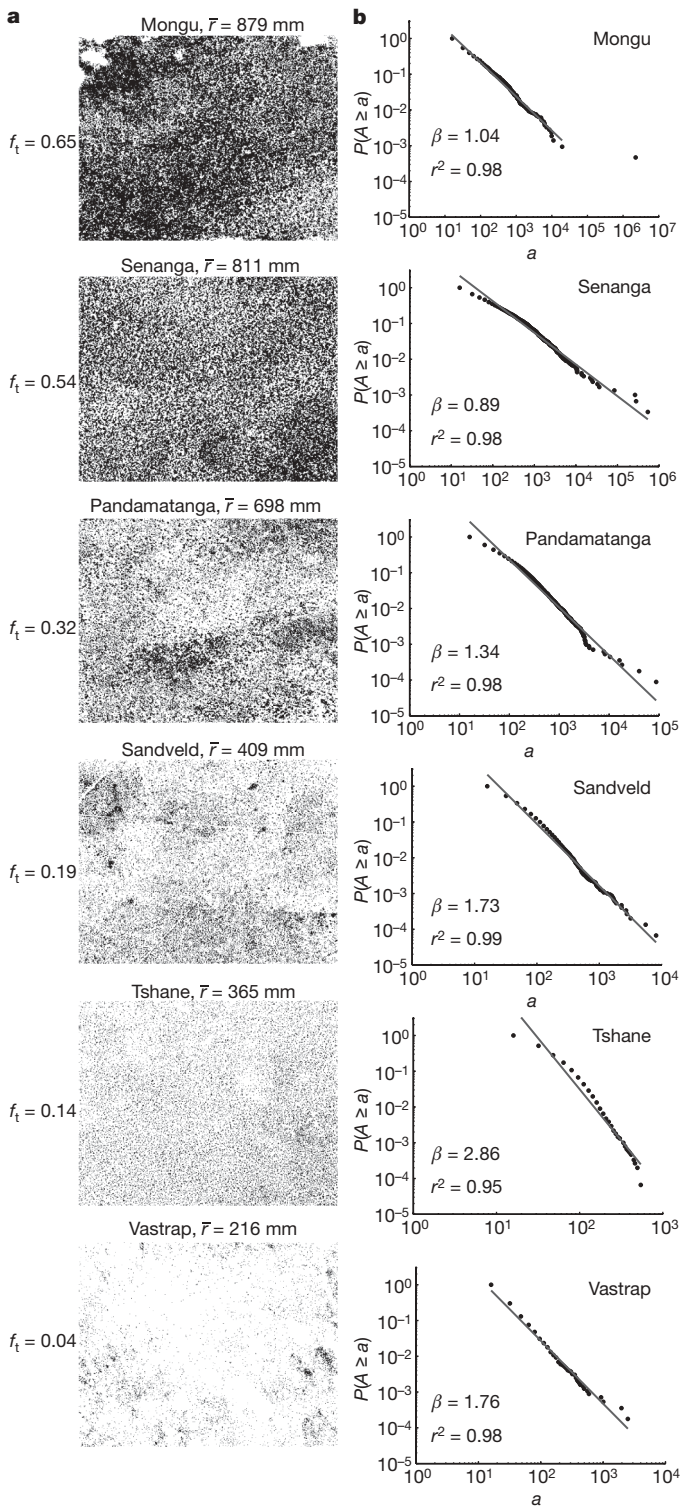
Figure 1 | Satellite observations of tree canopies and cluster size distributions. a, Binary data showing map views of the remotely sensed tree canopies, in which black points refer to the location of trees. The overall field of view is 2 km × 2 km, and the resolution is 4 m. Tree canopies were classified by thresholding the normalized difference vegetation index in the IKONOS scenes to match the fractional tree cover (f_t) measured in the field at each site. **b,** Cluster analysis of the tree canopy matrices, plotted as an inverse cumulative distribution on log–log axes. Power-law clustering is evident for a majority of the Kalahari sites, which vary widely in tree fractional cover along the rainfall gradient.

determine the size of contiguous clusters, we defined 'connected' tree pixels as those connected through any shared edge (that is, von Neumann neighbourhood; four immediate neighbours, no diagonals). In Fig. 1b, we provide the probability distribution for each of the six sites. These distributions demonstrate power-law relationships conforming to $P(A \geq a) \propto a^{-\beta}$ over a wide range of scales at all sites, with the possible exception of Tshane, where the cluster size distribution more closely resembles an exponential relationship. At the Mongu site, the single cluster that lies outside the power relationship corresponds to a cluster that spans the entire image being analysed. Power-law cluster size distributions such as these observed in the Kalahari have been cited as evidence of criticality[14], in which small perturbations to a forcing variable can lead to rapid and widespread changes to the ecosystem state (that is, savanna tree cover).

The ubiquity of power-law distributions of tree canopy cluster sizes merits further scrutiny. The coefficient of determination R^2 may be relatively high when fitting log–log relationships without any dynamic causality. In addition, percolation theory predicts the existence of power-law cluster size distributions for uniform random patterns at a fractional cover of approximately 0.59 for a square lattice with the von Neumann neighbourhood[15]. To determine the significance of our results and to provide a benchmark for our subsequent modelling analyses, we compare our observed distributions at each site to those produced by a neutral model[16]. The neutral model generates patterns by randomly assigning occupancy within a 500 × 500 matrix until the percentage of occupied pixels matches the overall site percentage cover. In this way, the neutral model matches the global constraint on tree cover, but contains no additional spatial processes. At each site we estimate the probability distribution function resulting from each of 1,000 simulations.

As shown in Table 2, the resulting random neutral models are largely unsuccessful in meeting the criteria of having both (1) an R^2 value greater than 0.98 (as exhibited by most of the satellite data), and (2) a size distribution spanning at least one and a half orders of magnitude. The latter condition was imposed to eliminate seemingly strong power-law relationships that can result from a deficiency of scales[17]. Cluster distributions derived from the satellite data demonstrate a tendency to form power-law distribution over a broad range of fractional covers, including at densities far from the percolation threshold (for more general fits to the satellite data, see Supplementary Table 3). The persistence of this scale-invariant tree pattern at sites along the Kalahari rainfall gradient begs a mechanistic understanding of the processes that lead to this emergent statistical property.

Power-law clustering has been observed in nature for a variety of phenomena, including mussel beds[18], forest gaps[19] and forest fires[20], and the pattern-formation processes for these systems have been evaluated through the implementation of lattice-based cellular automata models, in which complex system dynamics are represented by simple rules of interaction. What makes the present study distinct from these earlier findings is that the observed statistical pattern is maintained over an environmental gradient for a wide range of

Table 2 | Random neutral model versus cellular automata model.

		Random neutral model			Cellular automata model		
f_t	R^2_{obs}	$R^2 \geq 0.98$	a_{max}/a_{min} $> 10^{1.5}$	Both true	$R^2 \geq 0.98$	a_{max}/a_{min} $> 10^{1.5}$	Both true
0.65	0.98	802	1,000	802	849	1,000	849
0.54	0.98	0	1,000	0	944	1,000	944
0.32	0.98	0	1,000	0	993	1,000	993
0.19	0.99	0	0	0	701	1,000	701
0.14	0.94	605	0	0	652	1,000	652
0.04	0.98	455	0	0	577	969	577

Fits indicate the ability of models to produce power-law distributions, such as those detected from the satellite data. A total of 1,000 distributions were generated for each fractional cover. The number of model realizations in which the power law R^2 fit exceeded a threshold of 0.98 ($R^2 \geq 0.98$) and/or the distributions spanned at least one and a half orders of magnitude ($a_{max}/a_{min} > 10^{1.5}$) are provided.
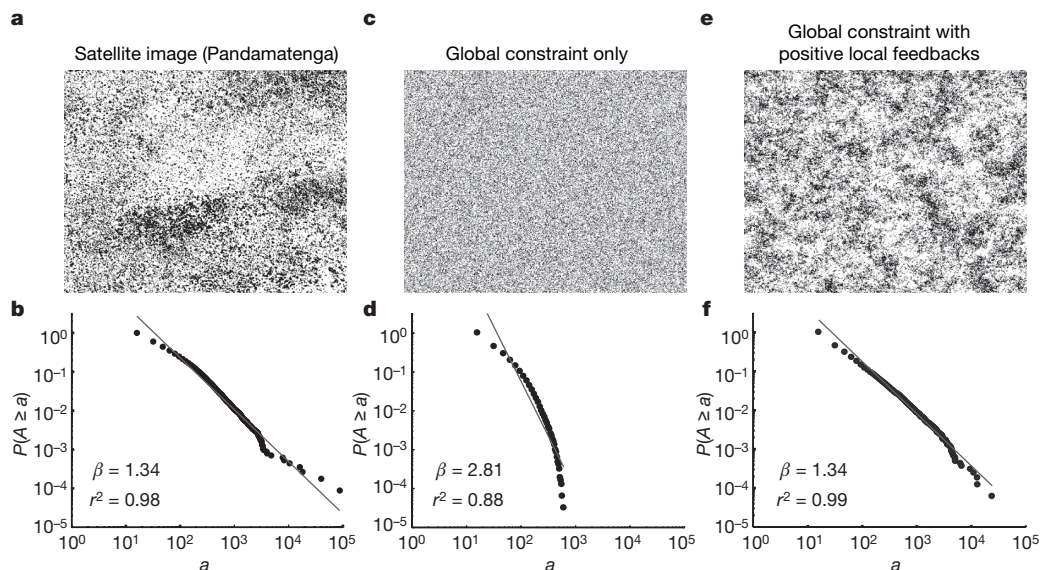
Figure 2 | Observations and models of tree canopy clustering. a, b, Satellite-observed tree cover for the Pandamatenga, Botswana site (**a**), and its inverse cumulative distribution that approximates a power-law fit (**b**). **c, d,** Spatial distribution of tree canopies produced by a random neutral model that considers only a global constraint on tree density (**c**), along with the inverse cumulative distribution (**d**), which approximates an exponential distribution of cluster sizes. **e, f,** Cellular automata-derived tree canopy distribution that accounts for both global constraints and positive local feedbacks on tree densities (**e**), with the scale-invariant distribution of cluster sizes resembling that of the satellite data (**f**).

vegetation densities. Any model capable of simulating the pattern-formation processes must meet the rigorous criteria of being strictly self-organizing (that is, no 'fine tuning' of parameters) and robust with respect to external environmental forcing. A recent survey of models used to produce power-law cluster size distributions in ecological systems[14] did not identify a general type that could satisfy the above conditions for a two-phase system (for example, presence/absence of trees). Disturbance-based models such as those typically used to describe power-law cluster formation do not seem to be realistic for the Kalahari setting. For instance, forest fire models[21], although capable of producing power-law cluster sizes, are not physically realistic because fire in this region is generally low-intensity and does not cause widespread mortality of trees[22].

Satellite observations and field surveys indicate that rainfall exerts a global control on tree density along the water-limited Kalahari Transect[12,23], whereas local interactions influence the spatial arrangement of individuals. A form of cellular automata model consistent with this framework is the Ising model of ferromagnetism, the two parameters of which account for global and local effects on transition dynamics. This model has previously been applied to reproduce an observed power-law gap size distribution in a neotropical forest[4]. Adapting the Ising model to account for the self-organized behaviour in the present case, however, is unsatisfactory given that it requires calibration to converge on power-law cluster size distributions. We therefore modified the model by linearizing the functional dependence of the transition probability on the neighbourhood and global structure, as well as by considering the influence of individuals beyond the von Neumann neighbourhood (see discussion in Supplementary Information). With no calibration, the model was capable of producing power-law cluster size distributions with $R^2 \geq 0.98$ at success rates of 57.7–99.3% for the six Kalahari Transect sites (Table 2). An example of the model output is shown in Fig. 2.

Power-law cluster size distributions are hallmarks of self-organization[24], and the consistent statistical pattern observed in the Kalahari points to internal feedbacks, rather than imposed spatial heterogeneity, in determining landscape-level vegetation distribution. An additional concept commonly associated with power-law cluster size distributions is criticality, which signifies a system poised at a phase transition[25]. This raises the question: is the Kalahari

ecosystem in a critical state such that small perturbations could result in rapid phase change (for example, desertification) from local interactions? This is highly unlikely, because disturbance propagation is required over relatively short timescales, and there is no physically based mechanism for this in the Kalahari. Furthermore, the model presented here exemplifies power-law formation in the absence of threshold behaviour and large, temporally intermittent fluctuations. If the dynamics were to be consistent at all with a critical state it would be with the kind of 'robust' criticality recently described[14]. Climate-driven phase transitions are possible in the Kalahari, but most likely are due to the global properties of the system through positive vegetation–climate feedbacks, as reported in the Sahel region of Africa[26].

We infer that the emergent spatial pattern in the Kalahari results from positive spatial feedbacks, in which the probability of establishment increases with local tree density, and the probability of mortality increases with greater open space in the vicinity of the tree. Water availability is hypothesized to be the main driver of these positive feedbacks, as below-canopy areas remain wetter in savanna ecosystems[27] owing to reduced bare soil evaporation from shading. Direct measurements of soil moisture at a number of locations along the Kalahari Transect have confirmed this general finding. Establishment is thus favoured in areas surrounded by trees, but this positive density-dependence can also be accounted for by seed dispersal[28] and nutrient availability[29], both of which are enhanced near existing tree canopies. Mortality brought on by water stress during dry years would be more pronounced for trees that do not have the benefit of neighbourhood shading, and increased lateral hydraulic gradients would deplete the soil moisture even further for these isolated individuals. Positive feedbacks of this type could lead to either desert or fully forested conditions[30], were it not for the density-independent global effect of rainfall. This, together with the distance-weighted local effects, leads to stable power-law cluster size distributions over a wide range of vegetation densities.

METHODS SUMMARY

The cellular automata model considers both local and global effects on transition probabilities between two states: tree canopy (t) and non-tree canopy (o). The local effect is governed by the neighbourhood tree density, ρ_t, which is weighted as a function of distance, d, away from the cell undergoing possible transition

according to a Pareto-type function. The spatial 'immediacy' of the neighbourhood effect is represented by the parameter k in the Pareto-like weighting $(d_{min}/d)^k$, where d_{min} is the minimum distance between cells in the model domain (4 m). A value of 3.0 was used for k in all simulations; this magnitude seems to affect β, but not the ability of the model to produce power-law cluster size distributions. The larger the value of k, the greater the weight placed on the tree density within the immediate vicinity of the cell in regard to its impact on ρ_t, which is defined as:

$$\rho_t = \sum_{\Omega_{i,j,M}} \left(d_{min}/d_{i,j}\right)^k x_{i,j} \Big/ \sum_{\Omega_{i,j,M}} \left(d_{min}/d_{i,j}\right)^k .$$

Here, $\Omega_{i,j,M}$ represents all positions i,j within a circular neighbourhood of radius M, and $x_{i,j}$ equals 1 for a tree canopy and 0 for non-tree canopy. The ability of the model to simulate power-law cluster size distributions is not contingent with the use of the Pareto weighting scheme; other functional forms representing diminished influence as a function of distance within the local neighbourhood are similarly efficient in generating power laws (see Supplementary Discussion).

The global effect on transition probability has the impact of aligning the overall fractional tree cover, f_t, with the fractional tree cover associated with the mean annual rainfall, $f_t^\star$, as determined by the observed linear relationship between these two variables. A linear combination between local and global effects yields the transition probabilities: $P(o \to t) = \rho_t + (f_t^\star - f_t)/(1 - f_t)$ and $P(t \to o) = (1 - \rho_t) + (f_t - f_t^\star)/f_t$. For each year of the simulation, 20% of the cells within the model domain were randomly selected for possible transition.

1. Solé, R. V. & Manrubia, S. C. Are rainforests self-organized in a critical state? *J. Theor. Biol.* **173**, 31–40 (1995).
2. Wooten, J. Local interactions predict large-scale pattern in empirically derived cellular automata. *Nature* **413**, 841–844 (2001).
3. Levin, S. A. The problem of pattern and scale in ecology. *Ecology* **73**, 1943–1967 (1992).
4. Katori, M., Kizaki, S., Terui, Y. & Kubo, T. Forest dynamics with canopy gap expansion and stochastic Ising model. *Fractals* **6**, 81–86 (1998).
5. Condit, R. *et al.* Spatial patterns in the distribution of tropical tree species. *Science* **288**, 1414–1418 (2000).
6. Asner, G. P. & Warner, A. S. Canopy shadow in IKONOS satellite observations of tropical forests and savannas. *Rem. Sens. Environ.* **87**, 521–533 (2003).
7. Cale, W. G., Henebry, G. M. & Yeakley, J. A. Inferring process from pattern in natural communities. *Bioscience* **39**, 600–605 (1989).
8. Aguiar, M. R. & Sala, O. E. Competition, facilitation, seed distribution and the origin of patches in a Patagonian steppe. *Oikos* **70**, 26–34 (1994).
9. Archer, S. Tree-grass dynamics in a Prosopis-thornscrub savanna parkland: reconstructing the past and predicting the future. *Ecoscience* **2**, 83–99 (1995).
10. Plotkin, J. B., Chave, J. & Ashton, P. S. Cluster analysis of spatial patterns in Malaysian tree species. *Am. Nat.* **160**, 629–644 (2002).
11. Koch, G. W., Scholes, R. J., Vitousek, P. M. & Walker, B. H. *The IGBP terrestrial transects: Science plan, Report No. 36* (International Geosphere-Biosphere Programme, Stockholm, 1995).
12. Scholes, R. J. *et al.* Trends in savanna structure and composition along an aridity gradient in the Kalahari. *J. Veg. Sci.* **13**, 419–428 (2002).
13. Caylor, K. K., Shugart, H. H., Dowty, P. R. & Smith, T. M. Tree spacing along the Kalahari Transect in southern Africa. *J. Arid Environ.* **54**, 281–296 (2003).
14. Pascual, M. & Guichard, F. Criticality and disturbance in spatial ecological systems. *Trends Ecol. Evol.* **20**, 88–95 (2005).
15. Stauffer, D. & Aharony, A. *Introduction to percolation theory* (Taylor and Francis, London, 1985).
16. Keitt, T. H. Spectral representation of neutral landscapes. *Landscape Ecol.* **15**, 479–493 (2000).
17. Halley, J. M. *et al.* Uses and abuses of fractal methodology in ecology. *Ecol. Lett.* **7**, 254–271 (2004).
18. Guichard, F., Halpin, P. M., Allison, G. W., Lubchenco, J. & Menge, B. A. Mussel disturbance dynamics: Signatures of oceanographic forcing from local interactions. *Am. Nat.* **161**, 889–904 (2003).
19. Manrubia, S. C. & Solé, R. V. On forest spatial dynamics with gap formation. *J. Theor. Biol.* **187**, 159–164 (1997).
20. Malamud, B. D., Morein, G. & Turcotte, D. L. Forest fires: An example of self-organized critical behavior. *Science* **281**, 1840–1842 (1998).
21. Grassberger, P. On a self-organized critical forest-fire model. *J. Phys. A* **26**, 2081–2089 (1993).
22. Holdo, R. M. Stem mortality following fire in Kalahari sand vegetation: effects of frost, prior damage, and tree neighbourhoods. *Plant Ecol.* **180**, 77–86 (2005).
23. Scanlon, T. M., Albertson, J. D., Caylor, K. K. & Williams, C. A. Determining land surface fractional cover from NDVI and rainfall time series for a savanna ecosystem. *Rem. Sens. Environ.* **82**, 376–388 (2002).
24. Pascual, M., Roy, M., Guichard, F. & Flierl, G. Cluster size distributions: signatures of self-organization in spatial ecologies. *Phil. Trans. R. Soc. Lond. B* **357**, 657–666 (2002).
25. Yeomans, J. M. *Statistical mechanics of phase transitions* (Clarendon Press, Oxford, 1992).
26. Wang, G. L. & Eltahir, E. A. B. Biosphere–atmosphere interactions over West Africa. II: Multiple climate equilibria. *Q. J. R. Metereol. Soc.* **126**, 1261–1280 (2000).
27. Scholes, R. J. & Archer, S. R. Tree–grass interactions in savannas. *Annu. Rev. Ecol. Syst.* **28**, 517–544 (1997).
28. Nathan, R. *et al.* Mechanisms of long-distance dispersal of seeds by wind. *Nature* **418**, 409–413 (2002).
29. Schlesinger, W. H., Reikes, J. A., Hartley, A. E. & Cross, A. F. On the spatial pattern of soil nutrients in desert ecosystems. *Ecology* **77**, 364–374 (1996).
30. Molofsky, J., Bever, J. D. & Antonovics, J. Coexistence under positive frequency dependence. *Proc. R. Soc. Lond. B* **268**, 273–277 (2001).

METHODS

Satellite data analysis. Several of the original 9 km × 9 km IKONOS scenes of the study sites contained cloud cover and noticeable human alterations to the landscape. We avoided these effects by limiting the vegetation pattern analysis to 2 km × 2 km subsampled areas that were representative of the surrounding landscape. Red and near-infrared channels of the IKONOS images, which have a resolution of 4 m, were used to construct 500 × 500 matrices of normalized difference vegetation index (NDVI). Field measurements of fractional tree cover[12] were used to threshold the NDVI, resulting in binary matrices of the tree cover (Fig. 1a). This methodology relies on the assumption that pixels with the highest NDVI correspond to tree canopies, and the thresholding procedure effectively filters out the between-canopy areas of grass and bare soil.

Cellular automata model implementation. All model runs were initiated with 50% fractional tree cover, randomly distributed throughout a 500 × 500 model domain. Ten model runs were performed for each of the six locations along the Kalahari Transect, characterized by their respective mean annual rainfall. After spin-up periods of 200 yr, cluster size distributions were evaluated from 'snapshots' of the model output each year over 100-yr timeframes (note that 'years' represents the model time step, which should not necessarily be equated with actual time evolution).

In the numerical implementation of the Pareto weighting scheme for the local density, a value of M was chosen such that the cumulative distribution function at this radius exceeded 0.999. A linear combination of local and global effects yields the transition probabilities. In rare cases when the calculated transition probability falls outside the range $\{0,1\}$, the probability is made equal to either 0 or 1.